

# A Novel Low Temperature Process for Microwave Dielectric Ceramics Metallization

Jau-Jr Lin<sup>1\*</sup>, Cheng-I Lin<sup>1</sup>, Tune-Hune Kao<sup>2</sup>, and Meng-Chi Huang<sup>2</sup>

<sup>1</sup>Department of Electrical Engineering  
National Changhua University of Education, Changhua County, 500, Taiwan, R.O.C.  
\*jaujrlin@cc.ncue.edu.tw

<sup>2</sup>Mechanical and System Research Laboratories  
Industrial Technology and Research Institute, Hsinchu County 310, Taiwan, R.O.C.

**Abstract** — This research proposes a novel low temperature process for microwave dielectric ceramics metallization with laser patterning and electroless copper plating. The process temperature of the proposed process is less than 50 °C, which is much lower than typical metallization technology, such as Low Temperature Co-fired Ceramics (LTCC) and Direct Bond Copper (DBC). Compared with LTCC and DBC, the proposed low temperature process can significantly reduce energy consumption, cut cost for cooling equipment, and offer smaller metal pattern variations. The measurement results demonstrate the line width error and the line position precision are all within ±50 μm. Moreover, this proposed process produces no short circuit or incomplete metallization in the walls of the holes. The measurement and simulation results demonstrate the manufactured samples meet the bandpass filter design specifications. Therefore, the proposed low temperature process is practical and adequate for producing microwave dielectric ceramics.

**Index Terms** — Ceramic laser metallization, laser engraving, microwave dielectric ceramics.

## I. INTRODUCTION

Microwave dielectric ceramics are the base material of important elements like filters, oscillators, antennas, and dielectric guides for mobile communications and consumer electronics products [1-6]. With the advance of mobile communications (4G, B4G and 5G), radio LAN (local area network), and GPS technologies in recent years, microwave elements based on microwave dielectric ceramics are being used more extensively and their demand has increased greatly. Therefore, the recent research is paying greater attention to fabricating microwave dielectric ceramics with less energy and manpower.

Conventional ceramic metallization technologies, such as Low Temperature Co-fired Ceramic (LTCC) and Direct Bonded Copper (DBC), are widely used nowadays. LTCC can fabricate three-dimensional ceramic modules with low dielectric loss and embedded silver electrodes [1, 2, 5]. Figure 1 illustrates the flow chart of the LTCC fabrication process. The ceramic tapes are blanked and then punched to create via holes. The next step is the via filling to form electrical interconnects between layers. Afterwards, screen printing or a photo image is used for metal patterning on each layer. The final steps are layer lamination and co-firing bellow 950 °C [1, 2, 5]. The dielectric constant, dissipation factor, and microwave resonance frequency of microwave components fabricated by LTCC are strongly correlated to the process temperature.

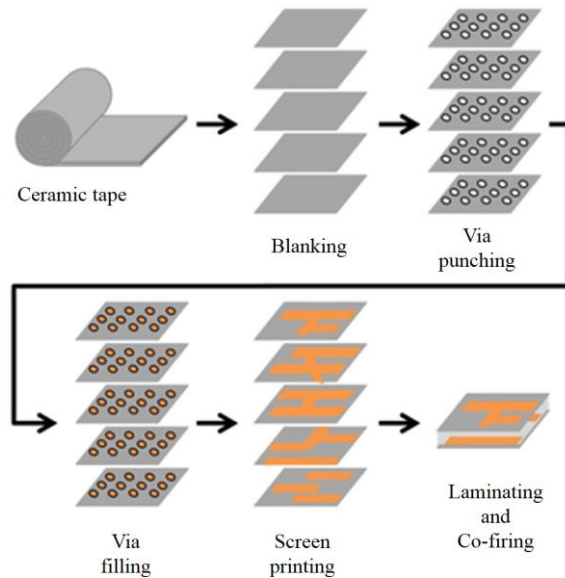


Fig. 1. The flow chart of the LTCC fabrication process.

DBC is the direct bonding process of copper and ceramics. The advantages of a DBC substrate are that copper metallization is relatively thick, and thermal expansion of the substrate near the surface is close to that of copper. Thus, copper and ceramic bonding strengths are high [7]. The oxygen concentration influences the bonding temperature of copper and substrate, such that when the oxygen concentration is 1.4%, the bonding temperature is a minimum 1065 °C [8].

For conventional ceramic metallization technologies, such as LTCC and DBC, screen printing or a photo image is utilized to generate the designated metal pattern. A silver paste or a copper paste is then employed. The whole ceramic substrate is sintered at a high temperature of 800-950 °C for more than one hour. In order to remove the polymer inside the silver paste or the copper paste, the whole ceramic substrate must be sintered at high temperatures for a long time to obtain good metal electrical properties. The entire process needs high energy and time consumption. Moreover, for the high-temperature sintering process, the metal pattern dimensions and position might show a deviation of 5-14% in error and might produce the aforementioned silver paste sticking or blockage, which causes short circuits or incomplete metallization in via holes. This will directly cause a resonant frequency offset of microwave dielectric ceramics. Due to undesired process variations, people need to inspect and calibrate individual devices one by one after the fabrication process, which requires much more time and labor to do.

A novel low temperature process for microwave dielectric ceramics metallization with laser patterning [9, 10] and electroless copper plating was therefore proposed to overcome those problems caused by the high temperature processes. This proposed process has several advantages over conventional LTCC process: lower energy consumption, less metal pattern dimension deviation, and no short circuit or incomplete metallization in via holes. The structure of the microwave dielectric ceramic and the detail of fabrication process are described and explained in the following sections.

## II. MICROWAVE DIELECTRIC CERAMICS

In the design stage, once specifications of the ceramic filter are given and finalized, the HFSS software is used for a preliminary simulation. The HFSS simulation setup is shown in Fig. 2. Figure 2 (a) shows the overall simulation set-up. Figure 2 (b) shows the details of the metal pattern and cavities. After the simulation results meet the filter specifications, the next step will be the fabrication process.

The microwave dielectric ceramic shown in Fig. 2 functions as a bandpass filter [3, 4, 6]. The equivalent circuit is shown in Fig. 3. The four resonant cavities in Fig. 2 can be modeled as the four LC parallel resonance circuits [3, 4, 6]. Here,  $L_x$  and  $C_x$   $\{x=1, 2, 3, 4\}$  are the

equivalent circuit for the four resonant cavities, shown in Fig. 3;  $C_{ij}$   $\{i,j = 0\sim 5\}$  represent the coupling capacitors between cavities and metal plates [3, 4, 6].

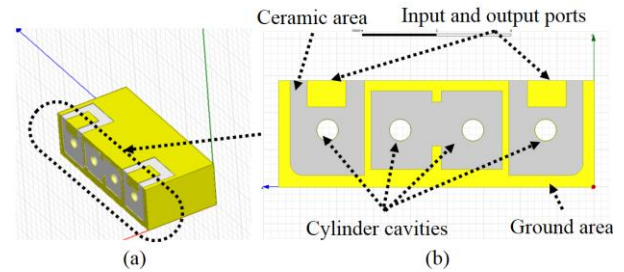


Fig. 2. HFSS simulation set-up.

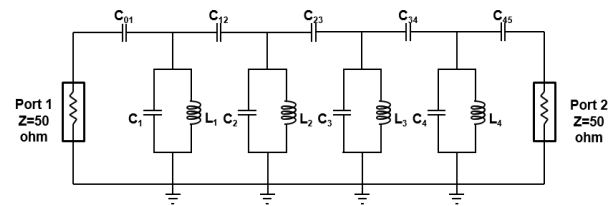


Fig. 3. Equivalent circuit of the filter.

From [11], the  $ABCD$  matrix of  $C_{ij}$   $\{i,j = 0\sim 5\}$  in Fig. 3 could be represented as equation (1), while the  $ABCD$  matrix of  $L_x$  and  $C_x$   $\{x=1, 2, 3, 4\}$  in Fig. 3 can be represented as equation (2). The total  $ABCD$  matrix is shown as equation (3) and can be transformed into the  $S$  matrix to obtain the reflection coefficients ( $S_{11}$  and  $S_{22}$ ) and transmission coefficients ( $S_{21}$  and  $S_{12}$ ):

$$\begin{bmatrix} A & B \\ C & D \end{bmatrix}_{C_{ij}} = \begin{bmatrix} 1 & \frac{1}{j\omega C_{ij}} \\ 0 & 1 \end{bmatrix}, \quad (1)$$

$$\begin{bmatrix} A & B \\ C & D \end{bmatrix}_{C_x \parallel L_x} = \begin{bmatrix} 1 & 0 \\ \frac{1}{j\omega L_x} + j\omega C_x & 1 \end{bmatrix}, \quad (2)$$

$$\begin{bmatrix} A & B \\ C & D \end{bmatrix}_{Total} = \begin{bmatrix} A & B \\ C & D \end{bmatrix}_{C_{01}} \begin{bmatrix} A & B \\ C & D \end{bmatrix}_{C_1 \parallel L_1} \begin{bmatrix} A & B \\ C & D \end{bmatrix}_{C_{12}} \cdots \begin{bmatrix} A & B \\ C & D \end{bmatrix}_{C_4 \parallel L_4} \begin{bmatrix} A & B \\ C & D \end{bmatrix}_{C_{45}}. \quad (3)$$

The geometric model of the microwave dielectric ceramic for the fabrication process is shown in Fig. 4, which is drawn by SolidWorks. There are four cylinder cavities for controlling the resonant frequency. The golden color areas are the designated metal patterns. There are two strip metal areas for the input and output ports. The other metal areas are for ground areas. The white area is the bare ceramic area. The overall dimension is about

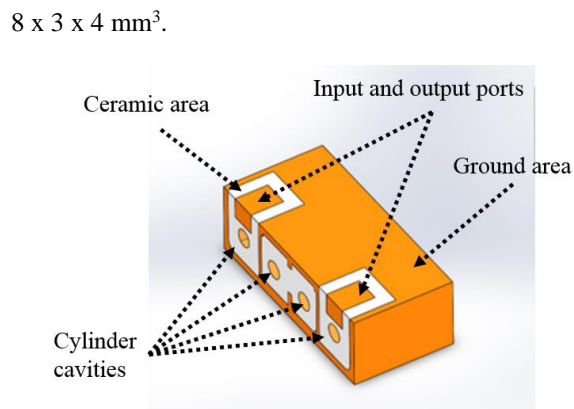


Fig. 4. The test structure of the microwave dielectric ceramic.

### III. PROPOSED FABRICATION PROCESS

The concept of the proposed low temperature process for microwave dielectric ceramics metallization is shown in Fig. 5. First, the ceramic substrate is trimmed to the desired dimension. The resonant cavities are created by punching. Second, the designated metal patterns are formed by applying ceramic laser metallization technology [9, 10]. By controlling the duration of electroless copper plating, the desired metal thickness can be obtained. Smart laser trimming [10] is utilized to trim the metal thickness on the surface of cavities to optimize the frequency response of the ceramic filter.

This research uses a perovskite-based ceramic as the substrate and applies the chemical deposition to form the metal patterns. Figure 6 shows the details of the ceramic metallization process. The component  $\text{CaTiO}_3$  is dissolved out of the ceramic by using an oxidative etching solution; e.g., phosphoric acid and HCl. Micro-pores are formed on the surfaces of ceramic and cavities. After this step, one can visually observe that the solution color is relatively yellow, as shown in Fig. 7 (a). According to the analysis of the dissolved etching solution, the solution contains Ca/Ti, proving that the etching solution roughens the surface. The ceramic is then kept in an activator for 10 minutes, as shown in Fig. 7 (b). The activator contains Sn and Pd ions, making the Sn and Pd ions adhere to the ceramic surface. It is kept in the cleaning agent for three minutes, as shown in Fig. 7 (c), with the purpose of cleaning off the Sn particles and leaving the Sn ions on the ceramic surface. Finally, the ceramic is put in a chemical copper solution, as shown in Fig. 7 (d). The chemical copper solution is heated with a water barrier for 1 hour, the temperature is adjusted between  $40\sim 50\text{ }^\circ\text{C}$ , and the deposition rate is around  $5\sim 7\text{ }\mu\text{m/hr}$ .

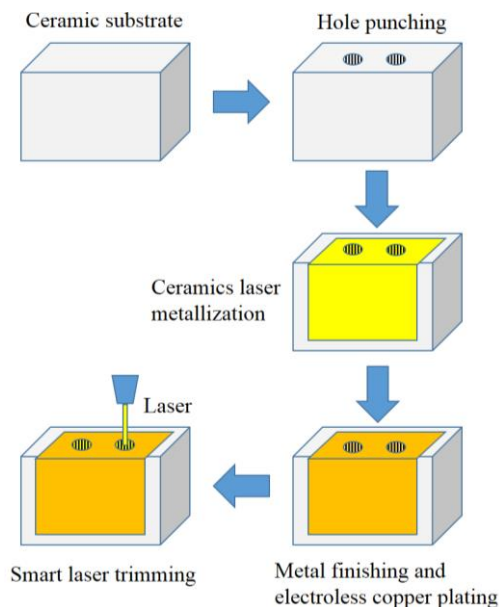


Fig. 5. Fabrication flow chart of the low temperature process for microwave dielectric ceramics metallization.

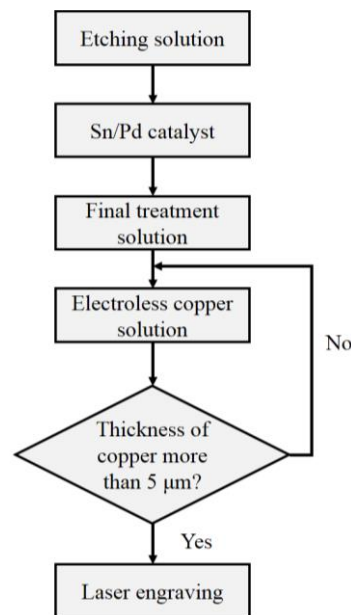


Fig. 6. The ceramic metallization process.

The laser engraving process is described here. First, the 3D geometric shape of the ceramic is built in a SolidWorks drawing software environment. The pattern to be processed by laser is then drawn, as shown in Fig. 2. The \*.step file is exported to a computer, and the ceramic height is adjusted to the laser processing height,

which is provided with a fixture and ceramic 3D model to make the computer correspond to the actual object. Next, the laser processing range is defined. Finally, the appropriate laser parameters are adjusted, such as wattage, frequency, speed, and times, so as to reduce the difference between the geometric model size and the size of laser engraving. The image registration is executed to remove the copper layer.

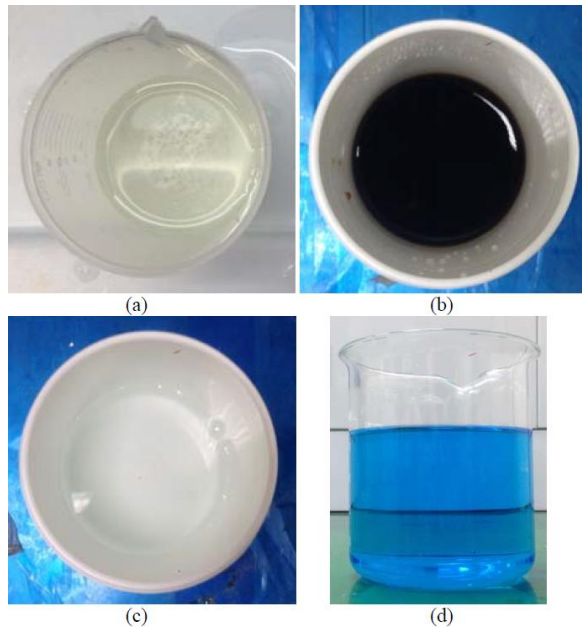


Fig. 7. (a) Etching solution, (b) activator, (c) cleaning fluid, and (d) chemically deposited copper solution.

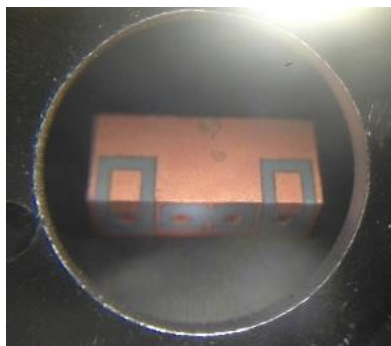


Fig. 8. Photo of the finished product.

#### IV. EXPERIMENTAL RESULTS AND DISCUSSION

The finished product after forming the chemically deposited copper and laser engraving is shown in Fig. 8. The picture is taken under the microscope. Table 1 shows

the error of line width after the proposed fabrication process. From Table 1, the line width errors are within  $\pm 50 \mu\text{m}$ , which are small and consistent through the three samples. Table 2 presents the error of the line's relative position. Once again, the error of the relative position of lines between the design and a final product are within  $\pm 50 \mu\text{m}$  and consistent through three samples. According to the comparison between the pattern and the laser engraving formed size, the line width and the relative position of the line are within  $\pm 50 \mu\text{m}$ ; as the screen plate is heated and used many times after, the error could be larger than  $100 \mu\text{m}$  [12].

Table 1: Line width errors between the original design and a final product

Line Width ( $\mu\text{m}$ )	Sample1 ( $\mu\text{m}$ )	Error ( $\mu\text{m}$ )	Sample2 ( $\mu\text{m}$ )	Error ( $\mu\text{m}$ )	Sample3 ( $\mu\text{m}$ )	Error ( $\mu\text{m}$ )
520	530	+10	533	+13	535	+15
310	324	+14	334	+24	335	+25
288.5	290	+1.5	297	+8.5	281	-7.5
260	281	+21	284	+24	281	+21
250	249	-1	246	-4	259	+9
180	195	+15	204	+24	191	+11
150	156	+6	139	-11	148	-2
120	121	+1	109	-11	114	-6

Table 2: The error of the relative position of lines between design and a final product

Relative Position of Lines ( $\mu\text{m}$ )	Sample1 ( $\mu\text{m}$ )	Error ( $\mu\text{m}$ )	Sample2 ( $\mu\text{m}$ )	Error ( $\mu\text{m}$ )	Sample3 ( $\mu\text{m}$ )	Error ( $\mu\text{m}$ )
1136	1111	-25	1120	-16	1129	-7
810	791	-19	793	-17	793	-17
750	719	-31	725	-25	719	-31
667	645	-22	648	-19	638	-29
630	603	-27	599	-31	604	-26
540	515	-25	511	-29	507	-33
460	426	-34	432	-28	441	-19

Figures 9 and 10 show the  $|S_{11}|$  and  $|S_{21}|$  comparisons among measurement data of the proposed process and the LTCC with screen printing process along with HFSS simulation results, respectively. As mentioned earlier, this ceramic filter structure is symmetric, and so here we only show the  $|S_{11}|$  and  $|S_{21}|$  data. According to the comparison among the S-parameters of the proposed process, the LTCC with screen printing process and the HFSS simulation results, the three of them have similar frequency bands and dB values. The measurement and simulation results demonstrate that the fabricated ceramic filter meets the specification requirements. Thus, the proposed low temperature process is practical and adequate for the microwave dielectric ceramics metallization applications.

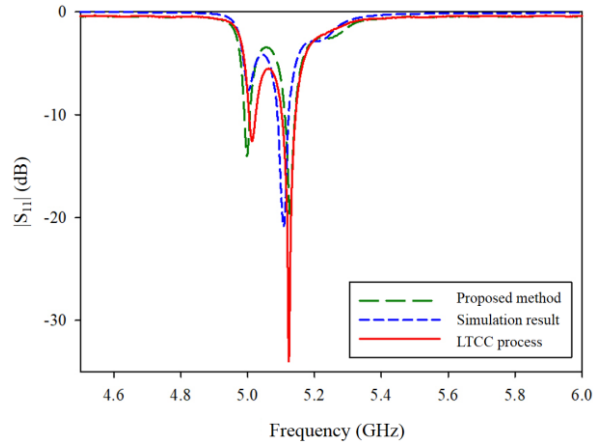


Fig. 9.  $|S_{11}|$  comparisons among measurement data of the proposed process and screen printing process and the HFSS simulation results.

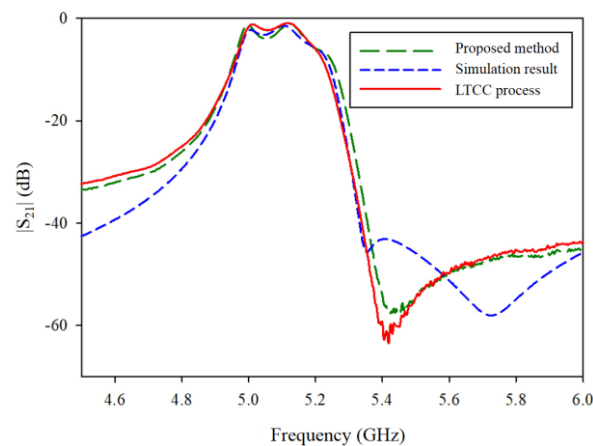


Fig. 10.  $|S_{21}|$  comparisons among measurement data of the proposed process and screen printing process and the HFSS simulation results.

Table 3: The comparison of process temperature during metallization among three methods: DBC, LTCC, and the proposed process

	LTCC [2]	DBC [7]	Proposed Process
Process temperature	900~1000 °C	1065 °C	< 50 °C

Table 3 shows the proposed method has the lowest process temperature among three methods. The entire process temperature of the proposed method is below 50 °C, which means that energy is saved significantly. Silver paste may stick to the screen due to re-use, and it will cause an error between the design and final product of more than 100  $\mu\text{m}$ . The proposed method, which applies an electroless copper plating process, can avoid

the silver paste stuck problem. Table 4 shows that the laser engraving has a smaller line width of 60  $\mu\text{m}$  than the LTCC with screen printing process and the line width error and relative position error are also within  $\pm 50 \mu\text{m}$ .

Table 4: The accuracy of proposed process and the LTCC with screen printing process

	LTCC with Screen Printing Process	Proposed Process
Minimum line width	100 $\mu\text{m}$	60 $\mu\text{m}$
Line width error	$\pm 100 \mu\text{m}$	$\pm 50 \mu\text{m}$
Relative position of lines	$\pm 100 \mu\text{m}$	$\pm 50 \mu\text{m}$

## VI. CONCLUSION

This research uses a perovskite-based ceramic to metallize microwave dielectric ceramics through chemically deposited copper. The temperature in the overall manufacturing process of the chemically deposited copper is below 50 °C. In comparison to other process methods, e.g., LTCC and DBC manufacturing processes, this technique can reduce the energy consumption effectively and greatly cut the cost of cooling equipment. In addition, the laser engraving forming technique can control the line width and relative position of the line more accurately. When screen printing is used repeatedly, the stuck silver paste exhibits dimensional discrepancy, leading to error signals. In addition, the metal may block up or incompletely adhere to the silver paste sintering pores; when each batch completed has to be checked, the labor cost increases. This study presents that the combination of chemically deposited copper and laser engraving can avoid the aforementioned silver paste sticking or blockage, and thus there is no short circuit or incomplete metallization in via holes. It can also effectively save energy and time when fabricating the appropriate microwave elements. The measurement and simulation results demonstrate that the fabricated ceramic filter meets the specification requirements. Thus, the proposed low temperature process is practical and adequate for the microwave dielectric ceramics applications.

## ACKNOWLEDGMENT

This research is supported by Mechanical and Mechatronics Systems Research Laboratories, Industrial Technology Research Institute (ITRI), Taiwan under Grant No. H301AR3400 and by the Ministry of Science and Technology, Taiwan, R.O.C. under Grant No. MOST 107-2221-E-018-002-. We are also grateful to the National Center for High-performance Computing (NCHC) for computer time and facilities.

## REFERENCES

- [1] R. R. Tummala, "Ceramic and glass-ceramic packaging in the 1990s," *Journal of the American Ceramic Society*, vol. 74, no. 5, pp. 895-908, 1991.
- [2] M. T. Sebastian and H. Jantunen, "Low loss dielectric materials for LTCC applications: A review," *International Materials Reviews*, vol. 53, no. 2, pp. 57-90, 2008.
- [3] C. Tang, C. Shen, and P. Hsieh, "Design of low-temperature co-fired ceramic bandpass filters with modified coupled inductors," *IEEE Transactions on Microwave Theory and Techniques*, vol. 57, no. 1, pp. 172-179, 2009.
- [4] M. Hoft and T. Shimamura, "Design of symmetric trisection filters for compact low-temperature co-fired ceramic realization," *IEEE Transactions on Microwave Theory and Techniques*, vol. 58, no. 1, pp. 165-175, 2010.
- [5] S. B. Narang and S. Bahel, "Low loss dielectric ceramics for microwave applications: a review," *Journal of Ceramic Processing Research*, vol. 11, no. 3, pp. 316-321, 2010.
- [6] J. Xu, X. Luo, L. Z. Cao, and R. S. Chen, "Optimization of coaxial dielectric resonator filter with aggressive space mapping," in *2012 Asia Pacific Microwave Conference Proceedings*, pp. 229-231, 2012.
- [7] J. Schulz-Harder, "Advantages and new development of direct bonded copper substrates," *Microelectronics Reliability*, vol. 43, no. 3, pp. 359-365, 2003.
- [8] T. Joyeux, J. Jarrige, J. Labbe, J. Lecompte, and T. Alexandre, "Oxygen influence on wetting and bonding between copper and aluminum nitride," *Key Engineering Materials*, vol. 206, pp. 535-538, 2002.
- [9] W. Li, M. Huang, T. Kao, W. Chung, and M. Chou, "Novel LIM (laser induced metallization) technologies of ITRI applied to WWAN/LTE 2-port antenna array for smart handset applications," in *2014 International Symposium on Antennas and Propagation Conference Proceedings*, 2014.
- [10] C. Yang, M. Chou, T. Kao, and M. Huang, "Applications of three dimensional laser induced metallization technology with polymer coating," in *2018 13th International Congress Molded Interconnect Devices (MID)*, 2018.
- [11] D. M. Pozar, *Microwave Engineering*. John Wiley & Sons, 2009.
- [12] J. Kita, A. Dziedzic, L. J. Golonka, and T. Zawada, "Laser treatment of LTCC for 3D structures and elements fabrication," *Microelectronics International*, vol. 19, no. 3, pp. 14-18, 2002.



**Jau-Jr Lin** received a B.S. degree from National Cheng Kung University, Taiwan in 1997, and a M.S. degree from National Chiao Tung University, Taiwan in 1999. He received a Ph.D. degree from the Department of Electrical and Computer Engineering, University of Florida, Gainesville, FL, U.S.A. in 2007. From 2007 to 2010, he was at Freescale Semiconductor Inc., Tempe, AZ, U.S.A., working on silicon-based millimeter-wave transmitters and millimeter-wave packages in 60-GHz wireless communication systems and 77/79-GHz automotive radar systems. From 2010 to 2012, he worked for Richwave Technology Corporation, Hsinchu, Taiwan as a Technical Section Manager, developing low-power wireless transceivers. In 2012, he joined the Department of Electrical Engineering at National Changhua University of Education, Changhua, Taiwan as an Assistant Professor, where his research interests are wireless communication systems, EM wave propagation, power systems, radar systems, RF circuits and antenna designs.